Aerosol and Air Quality Research, 16: 2119–2128, 2016

ISSN: 1680-8584 print / 2071-1409 online
doi: 10.4209/aaqr.2015.11.0633

Suppressive Effects of Silicon Dioxide and Diatomite Powder Aerosols on Coal Mine Gas Explosions in Highlands

Zhen-Min Luo[1*], Fang-Ming Cheng[1], Tao Wang[1], Jun Deng[1], Chi-Min Shu[1,2]

[1] School of Energy and Resources, Key Laboratory of Western Mine Exploitation and Hazard Prevention of Ministry of Education, Xi'an University of Science and Technology, 58, Yanta Mid. Rd., Xi'an 710054, Shaanxi, China
[2] Center for Process Safety and Industrial Disaster Prevention, National Yunlin University of Science and Technology, 123, University Rd., Sec. 3, Douliou, Yunlin 64002, Taiwan

ABSTRACT

A gas explosion is the severest threat to the safety of coal mines, particularly in highlands. For effectively preventing gas explosions in coal mines, a quartz tube–based gas explosion test system with an open end and a nearly spherically confined gas explosion testing device were devised, fabricated, and tested. The suppressive effects of aerosols, here silicone dioxide (SiO_2) and diatomite powder aerosols, of various sizes on mine gas explosions were studied. Scanning electron microscopy, low temperature nitrogen adsorption, and thermogravimetry analysis conducted on diatomite showed the porosity, effective specific surface area, adsorbability, and excellent thermal stabilities of the aerosols. Explosion suppression experiments confirmed that a test system of SiO_2 and diatomite powder aerosols remarkably prolonged the gas explosion induction period and the time of peak explosion pressure and reduced the flame propagation rate. In addition, the test system reduced the maximum explosion pressure and maximum and average explosion overpressure rising rates. The suppressive effects were clearly affected by the aerosol type and size. Microscale diatomite powder aerosol exhibited a stronger suppressive effect than microscale SiO_2 powder aerosol did. The porous structure and thermal characteristics of diatomite powder was vital in the suppression efficacy because they restrained the growth rate and activity of free radicals obtained through explosion reactions and eventually eliminated them. The adsorption of formaldehyde, a major intermediary of gas explosion, by diatomite powder decreased the quantity of free radicals, eventually suppressing explosions.

Keywords: Diatomite powder aerosol; Thermogravimetry analysis; Specific surface area; Peak explosion pressure; Flame propagation rate.

INTRODUCTION

In coal mining, ground air entering the mine forms mine air because of pollution. Similar to ground air, the main components of mine air are oxygen, nitrogen, and carbon dioxide. However, because of the influence of various natural factors and production processes, mine air also contains components such as dust and gas. In China's highlands, gas explosions are the leading accidents in underground coal mining. Gas concentration monitoring, gas accumulation prevention, non-fire source technology, and explosion suppression technology that reduces the influence range of an explosion are the main gas explosion prevention methods (Zhou, 2001). The first three approaches mainly prevent the simultaneous formation of the three elements necessary for a gas explosion, which are oxygen, proper concentration of gas and source of ignition. Futhermore, explosion suppression is mainly used when these three elements coexist. Through various techniques, suppression systems prevent the development of an initial explosion, hinder explosion flame propagation, alleviate the extent of damage, or curtail the extent of damage.

Common gas explosion suppressants include inert gases, which adding inert gas such as N_2, CO_2 and Ar to fuel-air reaction system to affect their explosion limits, critical oxygen concentration and explosion overpressure (Wang *et al*., 2008; Li *et al*., 2010; Jia *et al*., 2013).

Water mist has characteristics of low-cost and non-pollution. As its been generated by pressure devices, the pressure and diameter of nozzle combined with the size of water mist will have a great influence on the suppression effect. By adding the activators as NaCl, $NaHCO_3$, KCl and NaOH. the explosion suppression performance of water mist could be enhanced in some extent (Chelliah *et al*., 2002; Schwer and Kailasanath, 2007; Zhang *et al*., 2009; Gu *et al*., 2010; Yu *et al*., 2011). In addition, Yu *et al.* (2014) found that the charged

* Corresponding author.
Tel.: +86-029-85583142
E-mail address: luozm9903@163.com

water mist can effectively reduce the pressure peak of gas explosion and the propagation speed of flame than normal water mist, and with the increase of the charged voltage, the inhibiting effect of charged water mist on gas explosion is significantly enhanced.

For powder and aerosol-based explosion suppression technology (Mikhail, 2006; Krasnyansky, 2006; Luo *et al*., 2009; Wen *et al*., 2009; Jiang *et al*., 2010; Qu, 2010; Chen *et al*., 2011; Wang *et al*., 2012; Deng *et al*., 2012), ammonium phosphate derivatives (Wen *et al*., 2011a, b), alkali halide powders, carbonates (Chen *et al*., 2006; An *et al*., 2011), metal hydroxides, and refractory oxides (Wang *et al*., 2009; Wen *et al*., 2009) have been investigated as suppressants, finding the particle sizes, surface structures, and quantities of powder aerosol, the setting velocities and their thermal characteristics play key roles in suppressing process.

And in porous materials-based explosion suppression technology, Varying degrees of explosion inhibition have been realized using metal wire mesh, foamed ceramic, and porous foam metal suppressants (Ciccarelli *et al*., 2005; Joo *et al*., 2005; Zhang *et al*., 2012; Sun *et al*., 2013; Wei *et al*., 2013), finding bore diameters, thicknesses, densities, and components of porous materials are key factors affecting their gas explosion suppression efficacy.

Actually, the rock powder has the most wide range of application for explosion suppression in coal mines because of its' inexpensiveness and convenient to use. But its' suppressing effect is not optimal. SiO_2 powder is a typical aerosol widely used in industrial applications and is a common refractory raw material. Diatomite, a porous aerosol, is a biogenic siliceous sedimentary rock composed of the fossilized remains of diatom. Diatomite mainly contains SiO_2, with trace amounts of Al_2O_3, CaO, Fe_2O_3, K_2O, MgO, Na_2O, P_2O_5, and organic materials, rendering the diatomite exquisite, unconsolidated, light, and with excellent adsorption and immaculate osmosis characteristics. China is abundant in diatomite resources, with broadly distributed reserves of approximately 320 million tons and prospective reserves of approximately 20 million tons. Based on the comprehensive consideration of suppressing effect and the cost of suppressant in this study, methane, the dominant mine gas, was used as the experimental medium. Nanoscale and microscale SiO_2 powder aerosols and microscale diatomite powder aerosol were used as gas explosion suppressants, aiming to find some explosion suppressing powder that more effectiveness and accessible.

EXPERIMENTAL AND METHODS

Materials

SiO_2 (50-nm diameter; Haina Hi-Tech Materials Co. Ltd., Zibo, Jiangsu, China), SiO_2 (5-μm diameter; Hailong Powder Plant, Henan, China), and natural nanoscale diatomite (10-μm diameter; Xinghua Diatomite Fine Chemicals Co. Ltd., Linjiang, Jilin, China). The MASTERSIZER/E laser particle size analyzer made by Malvern Instruments was applied to test powder specification. Which results are shown in Fig. 1.

Experimental Systems

A self-designed quartz tube–based gas explosion test system named XKWB-S (Type S gas explosion system of Xi'an University of Science and Technology) and an XKWB-1 (Type 1 gas explosion system of Xi'an University of Science and Technology) cylindrical experimental system were used (Figs. 2 and 3) The quartz tube–based system comprised an explosion reaction pipe, an ignition control system, a gas explosion suppressant spraying system, and a multichannel high-speed data acquisition system (i.e., a high-speed camera). The explosion reaction vessel was a quartz tube with an inner diameter of 84 mm, total length of 1,600 mm, and effective volume of 8,860 mL. An igniter was placed in the blind end of the pipe, and the other end was sealed with a highly transparent polyethylene film. The high-speed camera placed within the pipe was 143 cm long. The entire experimental process was synchronously managed using the high-speed camera, which was activated as soon as methane was ignited. At 1,000 fps, the camera accurately captured a series of images of explosion flame propagation and completely demonstrated the changes in explosion flame propagation velocity in the pipe.

The XKWB-1 cylindrical experimental system comprised an explosion reactor and gas mixing, ignition, measurement, powder aerosol injection, and cleaning systems. The explosion reactor was a 20-L cylindrical vessel with an average diameter of 30 cm and an inner height of 35 cm. The measurement system mainly comprised a pressure sensor, a controller, and a computer. Data were collected from the moment that the igniter turned on. The response and maximum collection times were 1 and 500 ms, respectively. The pressure of compressed air was 1Mpa, the ignition energy was 1 J, and the delay time was 60 seconds. The experiments were conducted at temperature of 17.4–22.4°C and atmospheric pressure, with air humidity of 50–74% RH.

According to the experimental criteria of the American Society for Testing and Materials, an explosion occurs when the pressure increases by $\geq 7\%$.

EXPERIMENTAL RESULTS AND ANALYSES

Gas Explosion Induction Period

The gas explosion induction periods at different particle sizes of SiO_2 and diatomite powder aerosols are listed in Table 1. As shown in Fig. 4, the gas explosion induction periods varied with the type of aerosol. Increasing the powder aerosol concentration considerably increased the induction period. At a concentration of 11.28 mg L^{-1}, 10-μm diatomite, 5-μm SiO_2, and 50-nm SiO_2 powder aerosols extended the explosion induction period of 9.5% gas explosion by approximately four-, two-, and five-fold, respectively; 56.4 mg L^{-1} of nanoscale SiO_2 powder aerosol extended the gas explosion induction period by approximately 10-fold. The gas explosion induction period of microscale diatomite powder aerosol was longer than that of microscale SiO_2 powder aerosol. The induction periods of different aerosols were as follows: 5-μm SiO_2 < 10-μm diatomite < 50-nm SiO_2.

Characteristic Parameters of Explosion Flame Propagation

Using the length of the flame front between consecutive

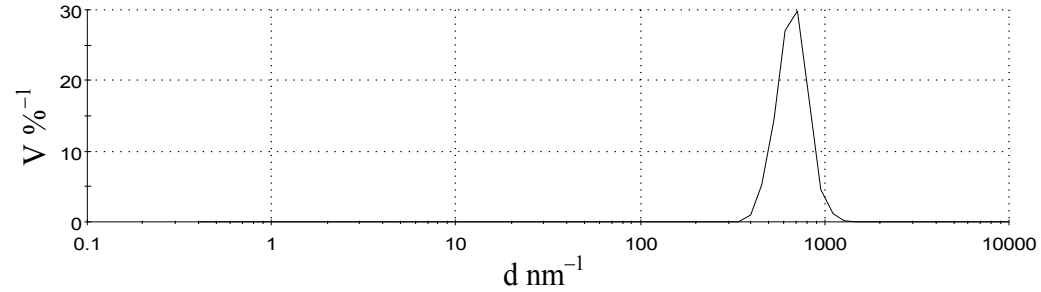

(a) Particle size distribution of 50-nm SiO_2 powder

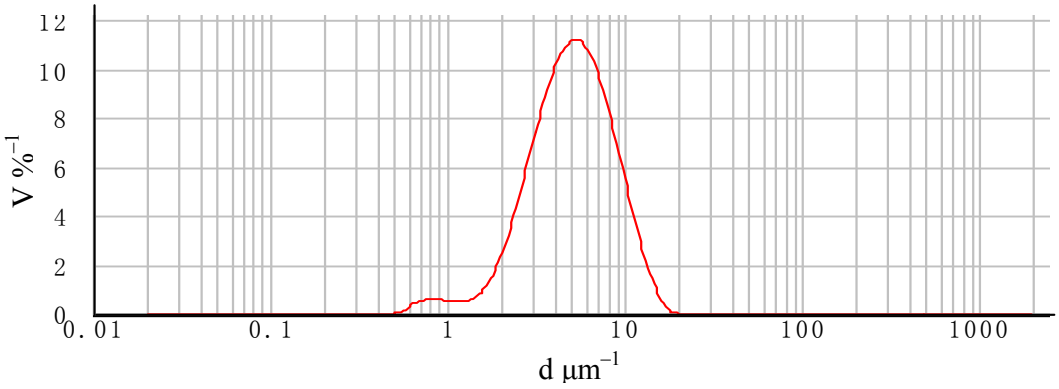

(b) Particle size distribution of 5-μm SiO_2 powder

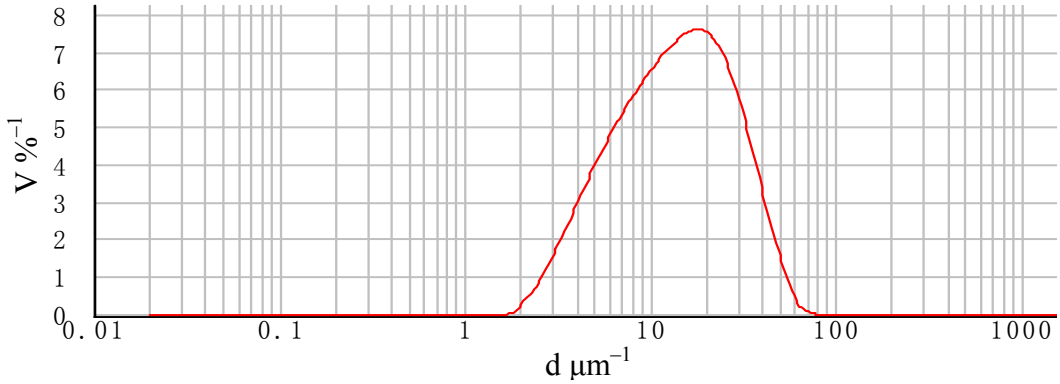

(c) Particle size distribution of 10-μm diatomite powder

Fig. 1. Particle size distribution of SiO_2 powder aerosol and powder aerosol.

high-speed photographs captured at 500 fps, the rates of explosive flames under different conditions were obtained. Because of wide variation in the starting points, the initiation point was unified for comparing the explosion flame propagation rate. Fig. 4 presents the effect of 11.28 mg L^{-1} of different aerosols on the explosion flame propagation rate. The propagation rate was considerably reduced by the addition of powder aerosols, particularly nanoscale SiO_2 powder aerosol. Changes in the explosion flame propagation rate after adding aerosols were more uniform than those in the absence of aerosols. Nanoscale and microscale powder aerosols exhibited nearly the same effect up to 42 ms; that is, explosion flame propagation rates slowly increased up to 34 ms, slowed down until 42 ms, and suddenly increased. Particularly, the explosion flame propagation rate accelerated after adding microscale SiO_2 powder aerosol. According to the changes in the explosion flame propagation rate, the explosion suppressive effects of the three aerosol types were as follows: 5-μm SiO_2 < 10-μm diatomite < 50-nm SiO_2.

The trends in changes of the flame propagation rates after adding different aerosols revealed that the flame propagation rate initially increased, decelerated, and subsequently peaked again after an inflection point. The flame propagation speed slowed down after peaking; however, when the flame nearly reached the top of the pipe, the speed increased again because of turbulence. Moreover, with decreasing particle size, the peak flame propagation speed considerably decreased and exhibited a decreasing trend. Accordingly, the explosion suppression effects of the three aerosol types were ranked as follows: 5-μm SiO_2 < 10-μm diatomite < 50-nm SiO_2. Peak flame speeds for 5-μm SiO_2, 10-μm diatomite, 50-nm SiO_2 were 56.7, 55.8, and 49.6 m s^{-1}, respectively. Compared with

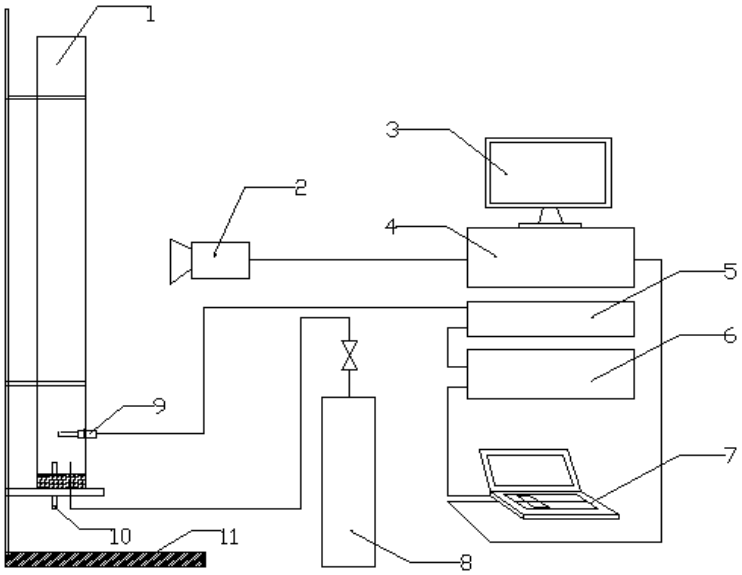

1-Quartz tube; 2-High-speed camera; 3-Displayer; 4-Data acquisition unit; 5-Igniter; 6-Controller; 7-Computer; 8-Gas cylinder; 9-Spark plug; 10-Suppressant spray entrance; 11-Fixed support

Fig. 2. Structure of XKWB-S quartz tube gas explosion test system.

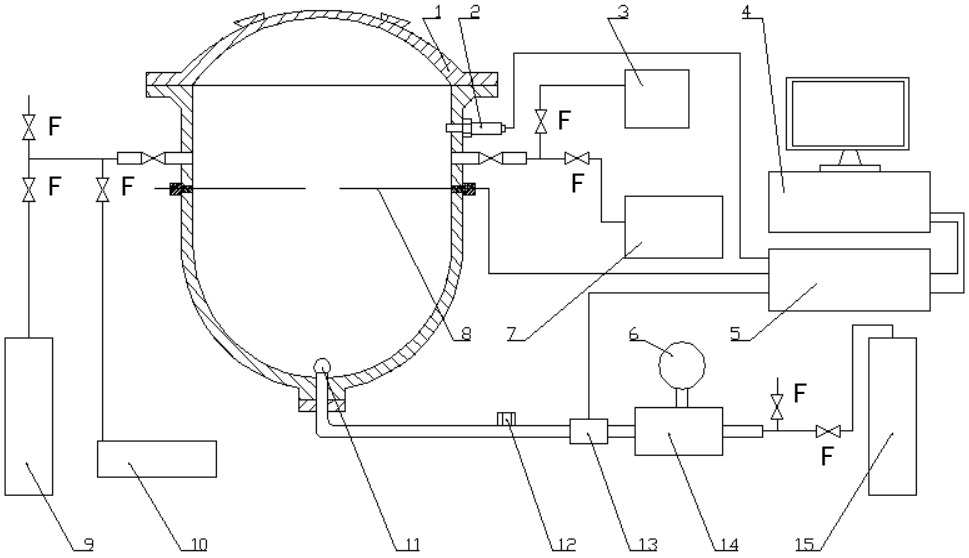

(a) 1-Explosion reactor; 2-Pressure sensor; 3-Digital pressure gauge; 4-Computer; 5-Controller; 6-Pressure gauge; 7-Vacuum pump; 8-Ignition source; 9-Methane cylinder; l0-Air compressor; 11-Powder aerosol injector; 12-Powder aerosol cylinder; 13-Solenoid valve; 14-High pressure air tank; 15-Compressed air cylinder

(b) The CY-DB1303 pressure sensor of experimental system (Range: 0–1 MPa, Response time: 1 ms, Accuracy: 0.3% F.S)

Fig. 3. Structure of XKWB-1 cylindrical experimental system.

Table 1. Explosion induction period of series powder aerosol.

Mass (mg L^{-1})	Without suppressant (ms)	5-μm SiO_2 (ms)	10-μm diatomite (ms)	50-nm SiO_2 (ms)
5.64		46	96	158
11.28	40	93	152	213
56.40		236	306	398

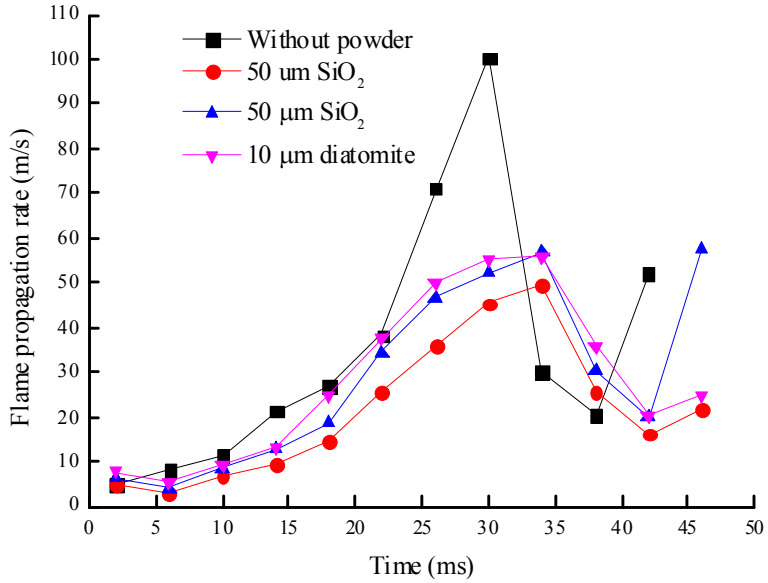

Fig. 4. Influence of 11.28 mg L^{-1} added amount of powder aerosol on flame propagation rate of gas explosion.

the flame speed in the absence of a powder aerosol, the speeds for 5-μm SiO_2, 10-μm diatomite, 50-nm SiO_2 decreased by approximately 44%, 45%, and 51%, respectively.

Characteristic Parameters of Explosion Pressure

The effect of various concentrations of nanoscale SiO_2 powder aerosol on the gas explosion pressure is shown in Fig. 5. The maximum explosion pressure and the pressure rising rate decreased with increasing aerosol concentration, and the explosion induction period and the time of peak explosion pressure were prolonged at powder aerosol concentrations < 100 mg L^{-1}. Nevertheless, at 150 mg L^{-1}, the maximum explosion pressure and the pressure rising rate increased and the explosion induction period and the time of peak explosion pressure decreased. Under the experimental conditions and at the optimal concentration of 150 mg L^{-1}, the nanoscale SiO_2 powder aerosol exhibited the optimal explosion suppression effect.

The effect of different types and particle sizes of aerosols (at 100 mg L^{-1}) on the gas explosion pressure is listed in Table 2. At 7% methane explosion, the maximum explosion pressure and the pressure rising rate apparently reduced and the explosion induction period and the time of peak explosion pressure were significantly prolonged. Therefore, among the suppressants used, nanoscale SiO_2 powder aerosol demonstrated the optimal suppressive effect for the experimental duration of 500 ms. At 7% methane explosion, nanoscale SiO_2 powder aerosol reduced the maximum explosion pressure, the pressure rising rate, and the average explosion rising rate by 71%, 76%, and 90%, respectively, and the time to reach the peak pressure was extended by more than three-fold. However, the suppressive effect of microscale diatomite powder aerosol was stronger than that of microscale SiO_2 powder aerosol. At 7% methane explosion, adding 5-μm SiO_2 powder aerosol reduced the maximum explosion pressure, the pressure rising rate, and the average explosion rising rate by 22%, 50%, and 72%, respectively, and the time to reach the peak pressure was extended by 2.8-fold. However, the suppressive effects of 5-μm SiO_2 powder aerosol were lower than those of 10-μm diatomite powder aerosol (30%, 58%, and 76%, and three- fold, respectively). Thus, the suppressive effect of SiO_2 and diatomite aerosol powders at the same concentration on 7% methane explosion was as follows: 5-μm SiO_2 < 10-μm diatomite < 50-nm SiO_2.

Suppression Mechanism

The results indicated that both SiO_2 and diatomite powder aerosols suppressed gas explosions. The suppressive effect of nanoscale SiO_2 aerosol powder was considerably stronger than that of microscale SiO_2 aerosol powder, whereas the suppressive effect of microscale diatomite aerosol powder was stronger than that of microscale SiO_2 aerosol powder.

Particle sizes and surface configurations of microscale SiO_2 and diatomite samples were recorded using a JSM-6460LV scanning electron microscope (SEM), and those of nanoscale SiO_2 sample were recorded using a JY/T010-1996 SEM. Low-temperature nitrogen adsorption experiments of the samples were performed using an ASAP2020 nitrogen adsorption instrument (Micromeritics Instrument Corp., Norcross, GA, USA), and thermogravimetric curves were

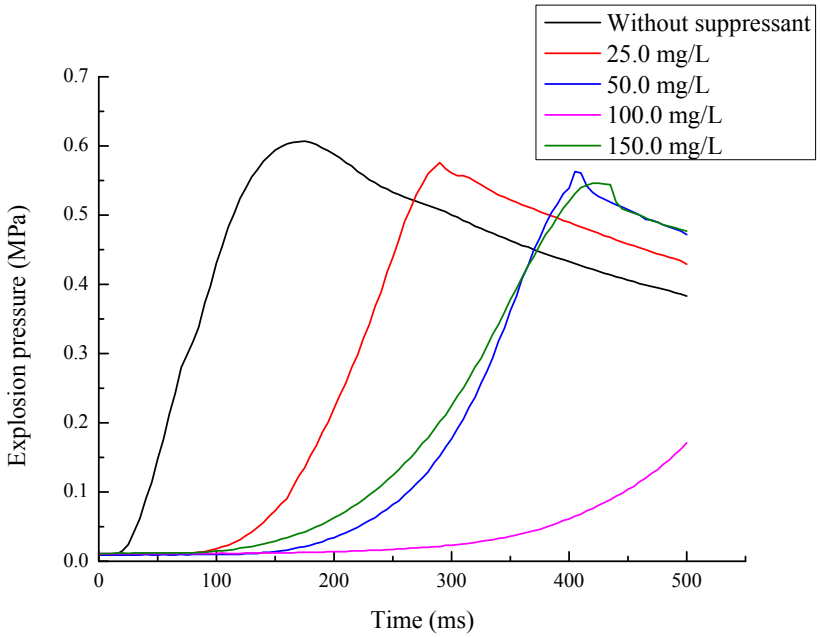

Fig. 5. Effect of nano-scale SiO_2 powder aerosol on 7% gas explosion pressure.

Table 2. Effect of different kinds and particle sizes of powder aerosol on gas explosion pressure at the concentration of 100 mg L^{-1}.

Sample	Maximum explosion pressure (MPa)	Maximum explosion pressure rising rate (Mpa s^{-1})	Average explosion rising rate (Mpa s^{-1})	Time to reach the peak pressure (ms)
Without suppressant	0.607	7.6	3.55	171
10-μm diatomite	0.428	3.2	< 0.86	> 500
5-μm SiO_2	0.477	3.8	1.01	473
50-nm SiO_2	0.179	1.8	< 0.36	> 500

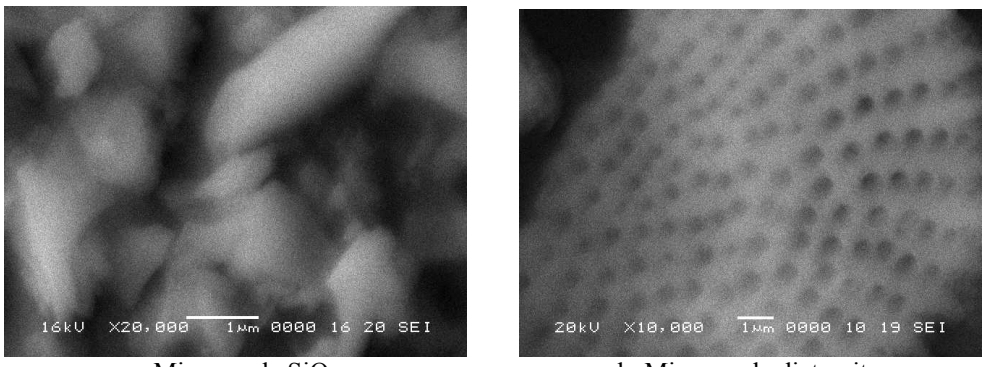

a. Micro-scale SiO_2 b. Micro-scale diatomite

Fig. 6. Photographs on micro-scales of SiO_2 powder aerosol and diatomite powder aerosol by SEM.

acquired using a thermogravimetry-differential scanning calorimetry simultaneous thermal analyzer (TG-DSC, Type 449C, produced by Netzsch).

Fig. 6 reveals that 1–5-μm microscale SiO_2 powder aerosol demonstrated a smooth surface. By contrast, nanoscale SiO_2 powder aerosols exhibited poor agglomeration on its flocculent surface. No porous structures were present on the surface of both materials. In fact, the prepared diatomite powder aerosol showed various particle shapes, such as rings, shells, and fans. A powder aerosol with porosity < 1 μm was uniformly distributed on the surface of each construction with aforementioned, that are rings, shells, and fans.

Low-temperature nitrogen adsorption results indicated that the specific surface area, microporosity, and average pore size of diatomite was 59.68 m^2 g^{-1}, 16.3%, and 9.254 nm, respectively, all of which contributed to its excellent adsorption performance.

Fig. 7 shows the TG-DSC curves of microscale and nanoscale SiO_2 and microscale diatomite in powder aerosols. Endothermic peaks caused by water loss from the samples

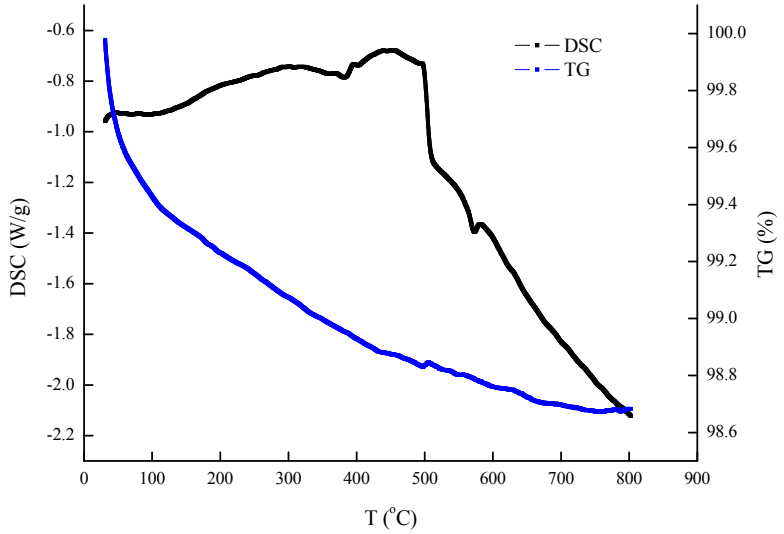

a. Micro-scale SiO_2

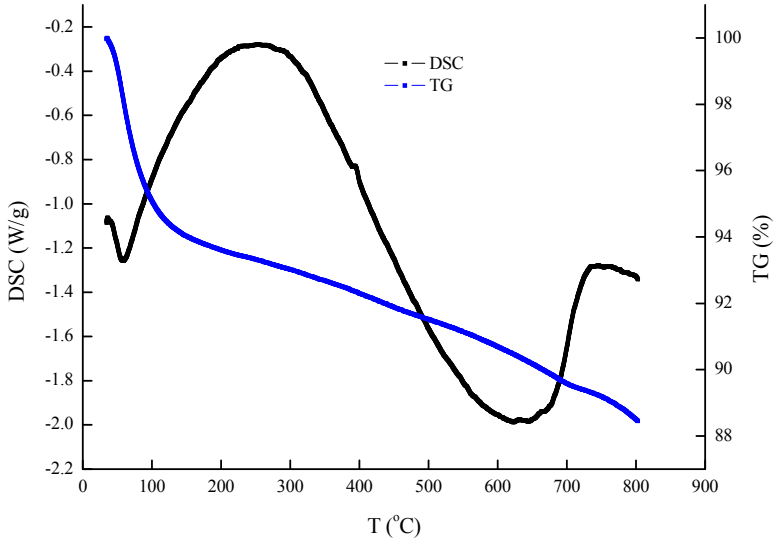

b. Nano-scale SiO_2

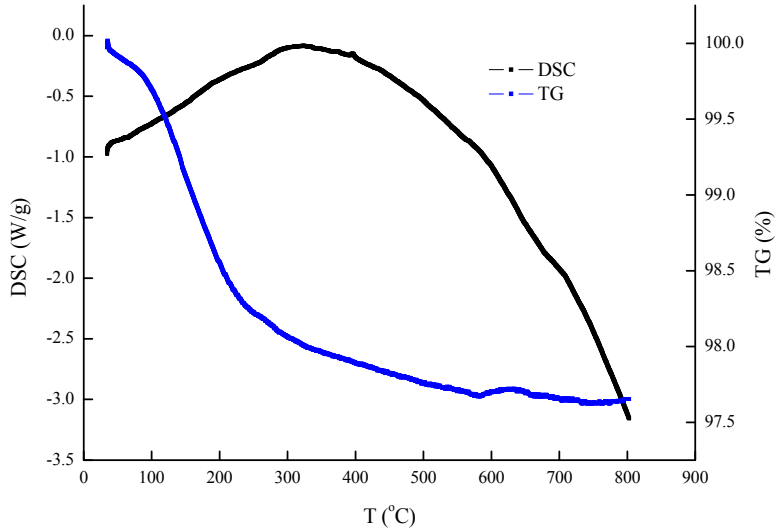

c. Micro-scale diatomite

Fig. 7. TG-DSC curves of samples (from 30 to 800°C).

were observed for microscale and nanoscale SiO_2 up to 120°C. Beyond 120°C, no obvious endothermic or exothermic peaks were observed, indicating the thermal stability of the tested materials. The thermal mass loss of nanoscale SiO_2 was more than that of microscale SiO_2, although both of them were similar in size. Because nanoscale SiO_2 has a larger specific surface area, which enhances water adsorbability, than microscale SiO_2 does, nanoscale SiO_2 contained slightly more water. The thermal mass loss of microscale diatomite occurred up to 425°C, and the TG curve was stable beyond 425°C. Thereafter, the mass loss of the diatomite sample during the experiment changed only from 100% to 97.8%, indicating its excellent thermal stability. The DSC curve of the microscale diatomite powder aerosol showed a clear endothermic peak between 50°C and 250°C, possibly because of the endothermic evaporation of water in the sample. The water may comprise bound and adsorbed water. At high temperatures, the bound water evaporated, causing the DSC endothermic peak to subside near 250°C. Moreover, other low-molecular-weight substances were considered to have decomposed during the aforementioned process, leading to fluctuations in the DSC curve.

Gas explosion was involved in a series of chain reactions, during which numerous free radicals with high reactivity capacity, such as O, $\dot{C}H_3$, $\dot{O}H$, $\dot{H}$, $H\dot{O}_2$, and $H\dot{C}O$, were generated. Inert additives catalyzed the decrease in the chain reactions (Xu *et al*., 2004) by converting the energetic free radicals to inactive radicals, slowing stable materials, or even terminating the free radical reactions. The explosion suppression mechanism of diatomite powder aerosol is as follows:

A. Slowing the Growth Rate of the free Radicals Involved in Explosion

According to Arrhenius reaction theory, decreasing temperature alleviates the rate of methane oxidation by hindering the free radical growth rate. The thermogravimetric curves of SiO_2 and diatomite powder aerosols showed that these aerosols lose the crystal or bound water and produce volatile substances through thermal decomposition for preventing explosion at a high temperature (2,000°C). These effects were achieved by absorbing an enormous amount of heat released from the combustion and explosion reactions, reducing temperature in the combustion and explosion zones, shortening the flame duration, and inhibiting explosion flame development. Furthermore, water vapor and volatile substances generated through decomposition diluted the concentration of methane and combustion air, thus stifling flame development. Solid particles separated methane and functioned as thermal radiators and conduction shields, effectively preventing gas explosion.

B. Weakening Free Radical Activity during Explosion

Because silicon powder particles and their solid phase decomposition products are inert solid particles, they can form an isolation layer for blocking combustion and explosion propagation in the explosion reaction zone as well as a barrier between activated molecules and free radicals. After the free radicals collided with inert solid particles, the energy of the radicals was transferred to the solid particles. Subsequently, the free radical activity disappeared, the responding ability of the system decreased, and the free radicals combined to form stable molecules. By contrast, after the inert solid particles collided with the free radicals, the radicals were instantaneously adsorbed on the particle surface and consumed by the particles. Therefore, the number of free radicals decreased sharply, thereby interrupting the gas explosion chain reaction.

C. Eliminating Free Radicals during Explosion

Low-temperature nitrogen adsorption and SEM analysis results revealed that the nanoscale SiO_2 powder aerosols were small and exhibited a surface effect caused by diatomite porosity. The atomic quantity and proportion on the surface increased rapidly, generating considerable surface energy, which made the atoms highly superficial, and the specific surface area increased sharply (150 $m^2 g^{-1}$). Moreover, because of coordination number inadequacy, many dangling bonds appeared. Particularly, porous materials adsorbed other atoms or chemically reacted with other atoms to render their surfaces in unsaturated fields for achieving a relatively stable state. Such unsaturation of nanoparticles enhanced the chemical activity and improved the adsorption capacity of the free radicals involved in explosion suppression. Small-particle powder aerosols heated up quickly and easily thermally decomposed or gasified, providing more sites for the free radicals generated in the reaction zone, which effectively reduces the quantity of free radicals and inhibits the gas explosion chain reactions.

Wang and Zheng (2011) reported that diatomite excellently adsorbs formaldehyde. $CH_2O + O_2 \rightarrow H\dot{O}_2 + H\dot{C}O$ is a crucial branched-chain reaction in methane explosion chain reactions and generates formaldehyde at temperatures less than 626.9°C. Thus, the diatomite decreased or eliminated the formaldehyde free radicals, which are essential components in gas explosion chain reactions. This finding was confirmed using the following quasi-steady method.

Because of the presence of H_2O, the product of gas explosion at temperatures less than 626.9°C, the total reaction rate of the explosion is as follows:

$$r_{CH_4} = \frac{d[H_2O]}{dt} = K_3 C_{CH_4} C_{\dot{O}H} + K_4 C_{CH_2O} C_{\dot{O}H} \quad (1)$$

According to the quasi-steady method, the reaction rates of intermediate products of gas explosion, such as $\dot{C}H_3$, $\dot{O}H$, $\dot{H}$, $H\dot{O}_2$, and $H\dot{C}O$, are as follows:

$$r_{\dot{C}H_3} = \frac{dC_{\dot{C}H_3}}{dt} = K_1 C_{CH_4} C_{O_2} - K_2 C_{\dot{C}H_3} C_{O_2} + K_3 C_{CH_4} C_{\dot{O}H} + K_7 C_{H\dot{O}_2} C_{CH_4} = 0 \quad (2)$$

$$r_{\dot{O}H} = \frac{dC_{\dot{O}H}}{dt} = K_2 C_{\dot{C}H_3} C_{O_2} - K_3 C_{CH_4} C_{\dot{O}H} - K_4 C_{CH_2O} C_{\dot{O}H} = 0 \quad (3)$$

$$r_{CH_2O} = \frac{dC_{CH_2O}}{dt} = K_2 C_{\dot{C}H_3} C_{O_2} - K_4 C_{CH_2O} C_{\dot{O}H} - K_5 C_{CH_2O} C_{O_2} - K_8 C_{H\dot{O}_2} C_{H_2O} = 0 \quad (4)$$

$$r_{\mathrm{H\dot{O}_2}} = \frac{dC_{\mathrm{H\dot{O}_2}}}{dt} = K_1 C_{\mathrm{CH_4}} C_{\mathrm{O_2}} + K_5 C_{\mathrm{CH_2O}} C_{\mathrm{O_2}} + K_6 C_{\mathrm{H\dot{C}O}} C_{\mathrm{O_2}} - K_7 C_{\mathrm{H\dot{O}_2}} C_{\mathrm{CH_4}} - K_8 C_{\mathrm{H\dot{O}_2}} C_{\mathrm{H_2O}} = 0 \quad (5)$$

$$r_{H\dot{C}O} = \frac{dC_{H\dot{C}O}}{dt} = K_4 C_{CH_2O} C_{\dot{O}H} + K_5 C_{CH_2O} C_{O_2} - K_6 C_{H\dot{C}O} C_{O_2} + K_8 C_{H\dot{O}_2} C_{H_2O} = 0 \quad (6)$$

From Eqs. (2)–(6), the following equations can be acquired:

$$2K_1 C_{CH_4} C_{O_2} + K_2 C_{\dot{C}H_3} C_{O_2} - K_4 C_{CH_2O} C_{\dot{O}H} + K_5 C_{CH_2O} C_{O_2} - K_8 C_{H\dot{O}_2} C_{H_2O} = 0 \quad (7)$$

$$2K_2 C_{\dot{C}H_3} C_{O_2} - K_3 C_{CH_4} C_{\dot{O}H} - K_4 C_{CH_2O} C_{\dot{O}H} - K_6 C_{H\dot{C}O} C_{O_2} = 0 \quad (8)$$

$$K_3 C_{CH_4} C_{\dot{O}H} + K_4 C_{CH_2O} C_{\dot{O}H} = K_6 C_{H\dot{C}O} C_{O_2} \quad (9)$$

Finally, Eq. (10) is obtained as follows:

$$r_{CH_4} = \frac{d[H_2O]}{dt} = K_6 C_{H\dot{C}O} C_{O_2} \quad (10)$$

where r is the reaction rate, C is the reactant concentration, and K is the elementary constant reaction rate.

Eq. (10) indicates that the quantity of $H\dot{C}O$ generated during gas explosion at low temperatures has a decisive role in explosions. Accordingly, eliminating $H\dot{C}O$ or preventing its formation effectively suppressed gas explosions. In addition, the porous diatomite powder aerosol used excellently adsorbed formaldehyde, effectively suppressing gas explosion.

CONCLUSIONS

A. Gas explosion suppression was clearly affected by the surface structure and particle size of aerosols, particularly in mines in highlands. SEM tests, low-temperature nitrogen adsorption examinations, and TG analyses were conducted on diatomite powder aerosol and its diatomite porosity, adsorbability, effective specific surface area, and excellent thermal stabilities were demonstrated. Compared with the diatomite powder aerosol, the SiO_2 powder aerosol, particularly the nanoscale SiO_2 powder aerosol with a small particle size and large specific surface area, exhibited a stronger suppressive effect. The suppressive effect of microscale diatomite powder aerosol was much stronger than that of microscale SiO_2 powder aerosol.

B. Results showed that the diatomite powder aerosol clearly prolonged the gas explosion induction period and the time of peak explosion pressure and reduced the maximum explosion pressure, the pressure rising rate, and the average explosion rising rate. Experiments conducted in the XKWB-S quartz tube–based gas explosion test system showed that 10-μm diatomite powder aerosol at 100 mg L^{-1} prolonged the induction period of 9.5% gas explosion approximately four-fold and decreased the flame peak speed by 45%. The XKWB-1 spherical experimental system was used for studying the suppressive effects of SiO_2 and diatomite powder aerosols on the pressure characteristics of gas explosion. The 10-μm diatomite powder aerosol reduced the maximum explosion pressure, the pressure rising rate, and the average explosion rising rate of 7% gas explosion by 30%, 58%, and 76%, respectively, and extended the time to reach peak pressure by more than three-fold.

C. The quasi-steady method was used for verifying the role of formaldehyde in gas explosions. The diatomite particles in aerosol excellently adsorbed formaldehyde, a reactant of the $CH_2O + O_2 \rightarrow H\dot{O}_2 + H\dot{C}O$ reaction that occurs in explosions. Thus, diatomite decreased or eliminated the quantity of formaldehyde free radicals.

D. The unique porous structure of diatomite increased the contact area available for the free radicals and the activated surface of the reaction-generating radicals, and enhanced the adsorption of free radicals during the explosion, markedly reducing the quantity of radicals. Thus, the explosion suppression effect of diatomite powder aerosol mainly relied on retarding the free radical growth rate in the explosion, weakening the free radical activities, and eliminating free radicals in the explosion reactions.

ACKNOWLEDGMENTS

The authors are thankful for the financial support from the National Natural Science Foundation of China (Grant Nos. 5090-4049 and 5130-4155), Key Science and Technology Program of Shaanxi Province (Grant No. 2015-SF280) and the Doctoral Fund of Xi'an University of Science and Technology (Grant No. 2013-QD-J048).

REFERENCES

An, A. (2011). Experimental study on inhibiting the gas explosion by water mist in tube, Thesis of Institutes of Technology of Henan, Henan, China (in Chinese).

Chelliah, H.K., Lazzarini, A.K., Wanigarathne, P.C. and Linteris, G.T. (2002). Inhibition of premixed and non-premixed flames with fine droplets of water and solutions. *Proc. Combust. Inst.* 29: 369–376.

Chen, X.K., Lin, Y. and Luo, Z.M. (2006). Experiment study on controlling gas explosion by water-depressant. *J. China Coal Soc.* 31: 603–606 (in Chinese).

Chen, X., Zhang, Y., Zhang, Q., Ren, S. and Wu, J. (2011). Experimental investigation on micro-dynamic behavior of gas explosion suppression with SiO_2 fine powders. *Theor. Appl. Mech. Lett.* 1: 032004.

Ciccarelli, G., Fowler, C.J. and Bardon, M. (2005). Effect of obstacle size and spacing on the initial stage of flame

acceleration in a rough tube. *Shock Waves* 14: 161–166.

Deng, J., Pu, G.M. and Luo, Z.M. (2012). Comparative experimental study on inhibiting gas explosion using ABC dry powder and diatomite powder. *J. Coal Sci. Eng.* 18: 138–142.

Gu, B.S., Wen, H.Y., Liang, Y.T. and Wang, X.Y. (2013). Mechanism characteristics of CO_2 and N_2 inhibiting methane explosions in coal mine roadways. *J. China Coal Soc.* 38: 362–366 (in Chinese).

Gu, R., Wang, X.S. and Xu, H.L. (2010). Experimental study on suppression of methane explosion with ultra-fine water mist. *Fire Saf. Sci.* 19: 52–59.

Guo, X.R. and Li, B.Z. (2002). Research on the use of ultra-fine diatomite as carrier. *Non-Metallic Mines* 25: 29–30 (in Chinese).

Jiang, X.S., Du, Y., Wang, D., Ou, Y.H., Wang, H.Y. and Liang, J.J. (2010). Research of fuel-air explosion suppressant based on ultra-fine cold aerosol. *J. Logistical Eng. Univ.* 26: 18–41.

Joo, H.I., Duncan, K. and Ciccarelli, G. (2006). Flame-quenching performance of ceramic foam. *Combust. Sci. Technol.* 178: 1755–1769.

Krasnyansky, M. (2006). Prevention and suppression of explosions in gas-air and dust-air mixtures using Powder aerosol-inhibitor. *J. Loss Prev. Process Ind.* 19: 729–735.

Li, C.B., Wu, G. D., Zhou, N. and Luo, Y. (2010). Numerical analysis of methane combustion suppression by $N_2/CO_2/H_2O$. *J. Univ. Sci. Technol. China* 40: 289–293 (in Chinese).

Luo, Z.M. (2009). Study of suppression materials' characteristics and effects on gas explosion. Xi'an University Science Technology Xi'an, Shaanxi, China (in Chinese).

Nie, B.S., He, X.Q., Zhang, J.F., Gu, X.M., Hu, T.Z. and Yang, C.L. (2008). Effect of foam ceramics upon gas explosion flame propagation. *Trans. Beijing Inst. Technol.* 28: 573–576 (in Chinese).

Qu, L.N. (2010). Experimental research on suppressing gas explosion by K and S-type aerosol. Xi'an University Science Technology Xi'an, Shaanxi, China (in Chinese).

Schwer, D.A. and Kailasanath, K. (2007). Numerical simulations of the mitigation of unconfined explosions using water-mist. *Proc. Combust. Inst.* 31: 2361–2369.

Sun, J.H., Li, Y.X. and Wei, C.R. (2013). Experimental study on the porous foam iron-nickel metal inhibition of gas explosion wave. *J. Funct. Mater.* 10: 1390–1394.

Wang, H., Ge, L.M. and Deng, J. (2008). Experimental study of using inert gas to suppress mine gas explosion. *Min. Saf. Environ. Prot.* 35: 4–7(in Chinese).

Wang, J. and Zheng, S.L. (2011). The Influence of acid-treating and calcination on adsorption properties to formaldehyde of diatomite. *Non-Metallic Mines* 34: 72–74 (in Chinese).

Wang, Q.H. (2009). Experimental research on suppressing gas explosion by ultrafine metal hydroxide powders. Thesis of Xi'an University of Science and Technology, Xi'an (in Chinese).

Wang, Q., Wen, H., Wang, Q. and Sun, J. (2012). Inhibiting effect of Al $(OH)_3$ and Mg $(OH)_2$ dust on the explosions of methane-air mixtures in closed vessel. *Sci. China Technol. Sci.* 55: 1371–1375.

Wei, C.R., Xu, M.Q. and Sun, J.H. (2012). Experiment and mechanism of porous materials for suppressing the gas explosion. *J. Funct. Mater.* 43: 2247–2255.

Wei, C.R., Xu, M.Q. and Wang, S.T. (2013). Experiment of porous materials for suppressing the gas explosion flame wave. *J. China Univ. Min. Technol.* 42: 006–213.

Wen, H., Wang, Q.H., Deng, J. and Luo, Z.M. (2009). Effect of the concentration of $Al(OH)_3$ ultrafine powder on the pressure of methane explosion. *J. China Coal Soc.* 34: 1480–1482 (in Chinese).

Wen, H., Cao, W. and Cheng F.M. (2011a). Experiment study on ultrafine ammonium phosphate dry powder to repress gas explosion. *Saf. Coal Mines* 42: 1–3.

Wen, H., Cao, W. and Wang K.T. (2011b). Experimental study on ABC dry powder to repress gas explosion. *J. Saf. Sci. Technol.* 7: 9–12 (in Chinese).

Xu, S.C. (2004). *Organic Chemistry*. Higher Educ. Press, Beijing, PR China (in Chinese).

Yu, J.L., Cai, T. and Li, Y. (2008). Experiment to quench explosive gas with structure of wire mesh. *J. Combust. Sci. Technol.* 14: 97–100 (in Chinese).

Yu, M.G., An, A. and You, H. (2011). Experimental study on inhibiting the Gas explosion by water spray in tube (in Chinese). *J. China Coal Soc.* 36: 418–422.

Yu, M.G., Liang, D.L., Xu, Y.L., Zheng, K. and Ji, W.T. (2014) Experimental study on inhibiting the gas explosion by charged water mist. *J. China Coal Soc.* 39: 2232–2238 (in Chinese).

Zhang, J.F., Wu, Y. and Liang, J.J. (2012). Effect of thermal conductivity of different pore foam ceramics' suppression of gas explosion. *Miner. Eng. Res.* 27: 44–48.

Zhang, Z., Gu, N., Cao, L. and Shu, X. (2009). Methane absorption and application of mixed organic aggregate prepared from span80 and alkaline salt. *Sci. China Ser. E: Technol. Sci.* 52: 2155–2160.

Zhou, S.N. (2001). *The Theory Strategy Research of Coal Mine Gas Disaster Prevention and Control*. China University Mining Technology Press, Xuzhou, Jiangsu, China (in Chinese).

Received for review, November 13, 2015
Revised, February 20, 2016
Accepted, February 22, 2016